Taylor & Francis
Taylor & Francis Group

Generation of calc-alkaline andesite of the Tatun volcanic group (Taiwan) within an extensional environment by crystal fractionation

J. Gregory Shellnutt[a]*, Alexander Belousov[b], Marina Belousova[b], Kuo-Lung Wang[c] and Georg F. Zellmer[d]

[a]Department of Earth Sciences, National Taiwan Normal University, Taipei, Taiwan; [b]Institute of Volcanology and Seismology, Petropavlovsk–Kamchatsky, Russia; [c]Institute of Earth Sciences, Academia Sinica, Taipei, Taiwan; [d]Soil and Earth Sciences Group, Massey University, Palmerston North, New Zealand

The Pliocene–Pleistocene northern Taiwan volcanic zone (NTVZ) is located within a trench-arc–back-arc basin and oblique arc–continent collision zone. Consequently the origin and tectonic setting of the andesitic rocks within the NTVZ and their relation to other circum-Pacific volcanic island-arc systems is uncertain. Rocks collected from the Tatun volcanic group (TTVG) include basaltic to andesitic rocks. The basalt is compositionally similar to within-plate continental tholeiites whereas the basaltic andesite and andesite are calc-alkaline; however, all rocks show a distinct depletion of Nb-Ta in their normalized incompatible element diagrams. The Sr-Nd isotope compositions of the TTVG rocks are very similar and have a relatively restricted range (i.e. I_{Sr} = 0.70417–0.70488; $\varepsilon Nd_{(T)}$ = +2.2 to +3.1), suggesting that they are derived directly or indirectly from the same mantle source. The basalts are likely derived by mixing between melts from the asthenosphere and a subduction-modified subcontinental lithospheric mantle (SCLM) source, whereas the basaltic andesites may be derived by partial melting of pyroxenitic lenses within the SCLM and mixing with asthenospheric melts. MELTS modelling using a starting composition equal to the most primitive basaltic andesite, shallow-pressure (i.e. ≤1 kbar), oxidizing conditions (i.e. FMQ +1), and near water saturation will produce compositions similar to the andesites observed in this study. Petrological modelling and the Sr-Nd isotope results indicate that the volcanic rocks from TTVG, including the spatially and temporally associated Kuanyinshan volcanic rocks, are derived from the same mantle source and that the andesites are the product of fractional crystallization of a parental magma similar in composition to the basaltic andesites. Furthermore, our results indicate that, in some cases, calc-alkaline andesites may be generated by crystal fractionation of mafic magmas derived in an extensional back-arc setting rather than a subduction zone setting.

Keywords: andesite; quaternary volcanism; Tatun volcanic zone; Taiwan; crystal fractionation

Introduction

Calc-alkaline andesite is a common volcanic rock found at ocean–continent and ocean–ocean convergent plate tectonic settings and is directly attributed to petrological processes that are inherent at subduction zone settings (Boettcher 1973; Miyashiro 1974; Ringwood 1974; Gill 1981; Davies and Stevenson 1992; Sisson and Grove 1993; Ulmer 2001; Poli and Schmidt 2002; Ernst 2010). The formation of andesitic magmas, including high-Mg andesite, may be related to either direct partial melting from a pyroxenitic mantle or to partial melting and mixing between melts derived from subducted oceanic crust and the overlying hydrated mantle wedge, with possible contributions from the crust during eruption (Arculus 1994; Kelemen 1995; Rapp *et al.* 1999; Shinjo 1999; Ulmer 2001; Poli and Schmidt 2002; Rudnick and Gao 2003; Zellmer *et al.* 2005; Kelemen and Yogodzinski 2007; Straub *et al.* 2008, 2011; Tatsumi *et al.* 2008; Chiaradia *et al.* 2011; Till *et al.* 2012). Therefore, the identification of calc-alkaline andesite in the geological record is used as evidence for the existence of ancient arc settings (Sheth *et al.* 2002). However, andesitic rocks are also found within extensional settings such as large igneous provinces and Archaean and Proterozoic greenstone belts, and may also be generated by fractional crystallization at shallow crustal levels or magma mixing; thus the identification of ancient calc-alkaline silicic rocks may not necessarily be indicative of a volcanic arc setting but rather a tensional (i.e. back-arc or continent rift) setting (Hawkesworth *et al.* 1995; Shinjo 1999; Sheth *et al.* 2002; Bryan 2007; Shellnutt and Zellmer 2010; Leclerc *et al.* 2011).

The northern Taiwan volcanic zone (NTVZ) is situated in a complicated tectonic setting involving interaction between the margin of East Eurasia and the Philippine Sea plate. The convergence of plates around the Ryukyu arc has created an instance where oblique arc–continental collision is occurring at the same site where a trench-arc–back-arc basin is forming (Suppe 1984; Teng 1990, 1996). Due to the nature of subduction beneath the Ryukyu arc and the oblique arc–continent collision, it is difficult to ascribe the appropriate tectonic setting to the Tatun volcanic group (TTVG) system, which is located at the northern

---

*Corresponding author. Email: jgshelln@ntnu.edu.tw

tip of Taiwan in the western portion of the NTVZ. Previous studies have suggested that the Tatun system may be subduction-related due to the identification of calc-alkaline andesitic rocks, whereas others suggest that it is related to back-arc rifting of the Okinawa trough (Chen 1975, 1978, 1990; Lo 1982; Juang 1993; Chung *et al.* 1995; Teng 1996; Chen and Teng 1997; Chen *et al.* 1999; Wang *et al.* 1999, 2004). The presence of basalts, which are compositionally similar to within-plate continental tholeiites, casts doubt on the volcanic arc interpretation (Chen *et al.* 1999; Wang *et al.* 1999, 2004).

Because of the complicated geological setting of the eastern NTVZ, the precise tectonic origin (i.e. convergent vs. divergent plate boundary) of the TTVG rocks remains uncertain but understanding the origin of the andesitic rocks and their relationship to the tholeiitic rocks may enable one to constrain the likely tectonic setting. In this study we present new major and trace elemental data and whole-rock Sr-Nd isotopes of the andesitic rocks from the TTVG of the northern Taiwan volcanic zone. Together with detailed geological observations and petrological modelling, we attempt to determine the likely origin of the andesitic rocks in order to provide insight into the eruptive tectonic setting of the TTVG.

Background geology

Taiwan is an active mountain belt created by the oblique collision between the northern Luzon arc and the Asian continent (Figure 1) (c.f. Teng 1990). Despite ongoing plate convergence in central and southern Taiwan, extensional collapse has occurred in the northern part of the mountain belt since the Pliocene–Pleistocene. Accordingly, Teng (1996) proposed a model for orogenic evolution of northern Taiwan, from mountain building by collision to subsequent extensional collapse, lasting only a few million years. The Quaternary northern Taiwan volcanic zone (NTVZ) comprises two major on-land volcanic fields, the Tatun and Keelung Volcano groups (TTVG and KLVG), two isolated volcanoes (Kuanyinshan (KYS) and Tsaolingshan) in the southwest, and several offshore volcanoes (Sekibisho, Kobisho, Pengchiayu, and Mienhuayu) in the northeast (Wang *et al.* 1999). Radiometric age dating shows that the NTVZ volcanism commenced at ~2.8–2.6 Ma and lasted throughout the Quaternary. The age dates suggest that the earliest eruptions occurred in the Sekibisho and Mienhuayu islets and the TTVG around 2.8–2.6 Ma, with the youngest ages around 0.2 Ma in most of the volcanic fields. In some localities, however, the volcanic ages might be younger than 0.2 Ma as dating results are close to or even smaller than the limit of the dating methods (Wang *et al.* 2004 and references therein). The NTVZ volcanic rocks consist dominantly of andesites with calc-alkaline geochemical characteristics, similar to those commonly observed in convergent-margin lavas

(Gill 1981; Belousov *et al.* 2010). Thus, they are regarded as the westernmost part of the Ryukyu volcanic arc (Chen 1990; Juang, 1993; Chung *et al.* 1995; Teng 1996). The conventional view was first questioned by Chen and Teng (1997), who suggested an extensional rather than a subduction regime for magma generation. To accommodate available geophysical and geological evidence, Wang *et al.* (1999) proposed that the NTVZ resulted from post-collisional extension related to the late Pliocene orogenic collapse of the northern Taiwan mountain belt (Teng 1996). The extension may also account for the reactivation of the opening of the Okinawa trough that commenced during the middle Miocene (Sibuet *et al.* 1995) but became inactive after the arc–continent collision in Taiwan. Reactivated rifting in the Okinawa trough began propagating to the southwest from ~1.5 Ma, with accompanying development of the westernmost part of the Ryukyu subduction system towards Taiwan (Chung *et al.* 2000).

Twelve samples (Table 1 and Figure 2), representing the youngest volcanic rocks erupted by the TTVG, were collected within the limits of the E–W volcanic ridge of the group from volcanic edifices that retained their primary volcanic landforms (i.e. minimal erosion) (Belousov *et al.* 2010). Notably older volcanic rocks of the SW–NE ridge of the TTVG are not considered in this paper but were discussed by Wang *et al.* (2004). Precise ages of the analysed rocks are not known, but the available $^{40}Ar/^{39}Ar$ age determinations of the sampled volcanoes suggest that these rocks are no older than ~300,000 years (Song *et al*. 2000a, 2000b; Chen *et al.* 2003). Radiometric ^{14}C dating of the youngest pyroclastic deposits of the area indicates that the final eruptions of the TTVG occurred at 23–13 ka, and possibly as late as 6000 BP (Belousov *et al.* 2010; Chen *et al.* 2010). Therefore it is conceivable that some of the analysed samples may have erupted during the early Holocene.

Ten of the studied samples represent lavas of the TTVG. Eight of these (166, T-223, 223a, 227, 229, 230, 249, 309) were collected from lava bodies having a coherent original shape clearly expressed in modern topography and, thus their source volcanoes are known. Two samples (210, 224) were collected from small outcrops and their source volcanoes are not well established. Most of the sampled flows were thick (tens to hundreds of metres), blocky lavas (they were very viscous when erupted); one sample (166) was collected from the steep-sided Shamao lava dome – it represents the most viscous variety of TTVG lavas; and one sample (309) represents a thin (1–2 m) flow of relatively fluid 'a'ā lava. Two samples (160, 190) represent juvenile rocks (blocks) from block-and-ash pyroclastic flows probably formed simultaneously with deposition of the youngest lava flows of Cising volcano. Stratigraphic relations of these pyroclastic flows indicate that these samples represent the youngest volcanic rocks of the TTVG (Belousov *et al.* 2010; Chen *et al.* 2010).
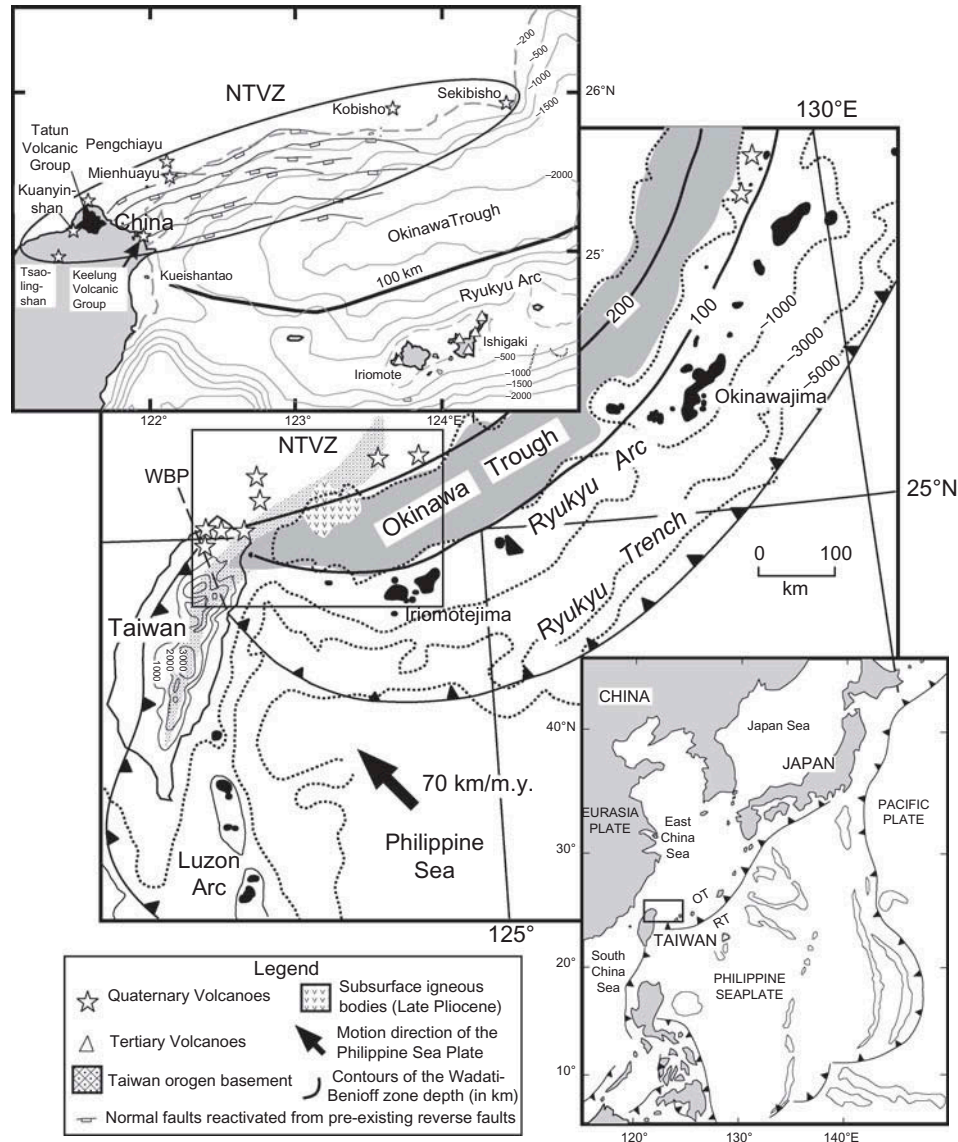
Figure 1.　Location and regional tectonic map (middle) of the northern Taiwan volcanic zone (NTVZ) in relation to the Eurasian and Philippine Sea plates (modified from Wang *et al.* 2004). The NTVZ is currently located ~200 km above the Wadti–Benioff zone. The stippled area is the basement of the Taiwan Orogen. The upper inset shows the bathymetry and detailed locations of the various volcanic edifies of the NTVZ. The 100 km contour is the surface projection of the depth to the Wadati-Benioff zone. The lower inset shows the regional tectonic setting of Taiwan. OT, Okinawa Trough, RT, Ryukyu trench.

Table 1.　Sample location and rock types of the Tatun volcanic group.

| Point	Volcano	Latitude	Longitude	Deposit	Composition
160	Cising	25° 9′26.60″N	121°34′1.20″E	Pf of Cising	Andesite
166	Shamao	25° 8′44.77″N	121°32′52.64″E	Lava dome	Andesite
190	Cising	25° 8′52.00″N	121°32′58.00″E	PF of Cising	Andesite
210	Siaocao	25° 8′26.90″N	121°32′31.00″E	Blocky lava flow	basaltic andesite
223	Wanli	25°10′46.48″N	121°40′26.58″E	Blocky lava flow	basaltic andesite
224	Wanli	25° 9′55.50″N	121°40′17.00″E	Blocky lava flow	basaltic andesite
227	Huangzuei	25°11′20.50″N	121°36′47.20″E	Blocky lava flow	basaltic andesite
229	Huangzuei	25°11′55.80″N	121°35′49.50″E	Blocky lava flow	basaltic andesite
230	Huangzuei	25°11′30.30″N	121°36′25.00″E	Blocky lava flow	basaltic andesite
249	Siaocao	25° 6′22.62″N	121°32′9.16″E	Blocky lava flow	basaltic andesite
309	Hunglu	25°11′49.30″N	121°30′34.20″E	'a'ā lava flow	basalt

Note: Pf, pyroclastic flow.
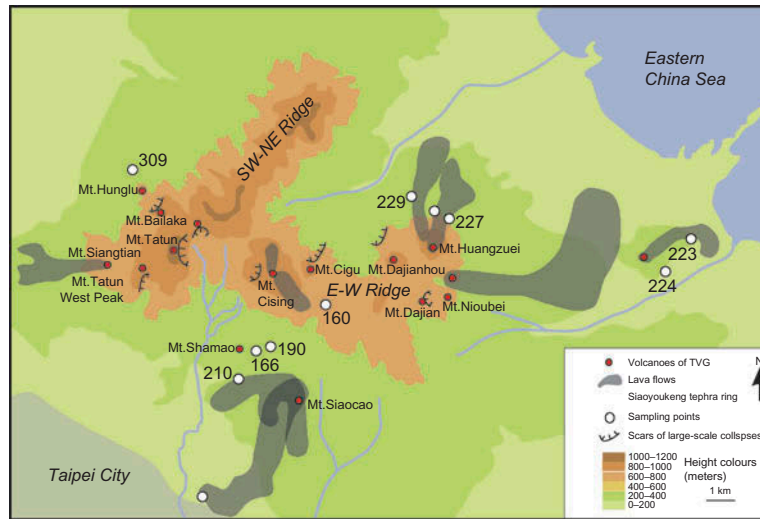
Figure 2. Sketch map of Tatun volcanic group, northern Taiwan, showing points where the analysed samples were collected. Locations of the main volcanic ridges, volcanoes, lava flows, and collapse scars are indicated. Transliteration of main topographic names from Chinese into English can be found in Table 1 (Belousov *et al.* 2010).

Petrography

The basalt sample (309) from Hunglu is fresh and consists of phenocrysts of olivine (≤5% vol.%), clinopyroxene (15–20 vol.%), and plagioclase (25–30 vol.%) within a fine-grained groundmass (40–50 vol.%). The rounded olivine crystals vary in size from 0.1 to 1.0 mm and tend to form agglomerates. The clinopyroxene crystals are typically euhedral to subhedral and can be up to 2 mm in size. The plagioclase crystals are euhdral but have variable shapes ranging from tabular to blocky. The majority of the basalt is a fine- to very fine-grained groundmass, some of which is composed of plagioclase and clinopyroxene whereas the remainder cannot be readily identified under the microscope. There is a small portion of opaque minerals identified as Fe-Ti oxides (i.e. <5 vol.%).

The basaltic andesites comprise two groups. The first group (i.e. 229, 230, 249) consists of phenocrysts (length 0.1–3.0 mm length) of olivine (<5 vol.%), pyroxene (~10 vol.%, mostly clinopyroxene), and plagioclase (30–40 vol.%). A fine- to very fine-grained groundmass comprises ~50–60 vol.%. The olivine crystals are rounded in shape whereas the pyroxenes tend to be euhedral. The plagioclase crystals are euhedral with shapes aligned with the 010, 110, and 001 crystal faces and show chemical zonation. The only minerals that can be identified in the groundmass are plagioclase, pyroxene, and a small amount (i.e. <2 vol.%) of euhedral to anhedral Fe-Ti oxides. The second group of basaltic andesites (223, 223a, 224) is not as fresh and contains pyroxene (~5 vol.%), plagioclase (~25 vol.%), and amphibole (25 vol.%) within a very fine-grained groundmass (~40 vol.%). The pyroxene is euhedral to anhedral, with some crystals altering to amphibole. The original plagioclase crystals show chemical zonation and are typically euhedral but in many cases are breaking down to clay minerals. There are two different amphibole crystals in the rock, both euhedral to anhedral, but one is distinctly dark brown to tan in plane polarized light whereas the other is clear and has a low to moderate relief. The dark brown amphibole may be oxy-hornblende whereas the clear amphibole may be cummingtonite. The mineralogy of the matrix cannot be reliably identified. It appears that the second groups of basaltic andesites have a more evolved mineral assemblage and seem to have experienced magmatic hydrothermal alteration.

The andesites (160, 166, 190) are relatively fresh and fall within the region attributed to the hornblende two-pyroxene (Lo 1982). The andesites contain phenocrysts of pyroxene (~15 vol.%, mostly clinopyroxene), plagioclase (~30 vol.%), and hornblende (10–15 vol.%) within a fine-grained to very fine-grained matrix (~40–50 vol. %). The pyroxene crystals, both clinopyroxene and orthopyroxene, are euhedral to anhedral. Some crystals are altering to amphibole. The plagioclase crystals are euhedral to subhedral with shapes similar to those observed in the basaltic andesites. In some cases the plagioclase crystals are altering to clay minerals. The hornblende crystals are euhedral to anhedral and show variably altered texture. The volume percentage of hornblende can vary considerably within the rock. Plagioclase is the only silicate mineral that can be identified within the matrix but there are also some Fe-Ti oxides present. Lo (1982) reported that some andesites from the southern margin of the E–W ridge area have been altered by volcanic degassing (i.e. H_2O and SO_2).

Analytical methods

Wavelength dispersive x-ray fluorescence spectrometry (WD-XRFS)

The samples were cut into small pieces using a diamond-bonded steel saw and were then crushed in a steel jaw crusher. The crusher was extensively cleaned after each sample with de-ionized water. The crushed samples were pulverized in an agate mill until a suitable particle size was obtained. The samples were heated to temperatures of ~110 and ~900°C to determine loss on ignition (LOI). Lithium metaborate was added to the oxidized samples and fused to produce a glass disc using a Claisse M4 fluxer. The major oxide concentrations were determined by WD-XRFS using a PANalytical Axios mAX spectrometer at the National Taiwan Normal University in Taipei. The long-term precision for SDC-1 standard reference material on 30 analyses is better than ± 0.5% for all elements except MgO, Na_2O, and P_2O_5, which is better than ±2% (Table 2). The long-term precision for BIR-1 standard reference material on 39 analyses is better than ±0.5% for all elements except Na_2O and K_2O, which is ±2% (Table 2).

ICP-MS trace element geochemistry

Whole-rock trace elemental analysis was conducted at Activation Laboratories, Ancaster, Ontario, Canada using the total digestion ICP method. A 0.25 g sample is digested with four acids beginning with hydrofluoric, followed by a mixture of nitric and perchloric acids. This is then heated using precise programmer-controlled heating in several ramping and holding cycles, which takes the samples to incipient dryness. After attaining incipient dryness, samples are brought back into solution using aqua regia. With this digestion, certain phases may be only partially solubilized; these phases include zircon, monazite, sphene, gahnite, chromite, cassiterite, rutile, and barite. The samples are then analysed using an Agilent 735 ICP. Quality control, for which the digestion is 14% for each batch, 5 method reagent blanks, 10 in-house controls, 10 sample duplicates, and 8 certified reference materials (Table 2). An additional 13% quality control is performed as part of the instrumental analysis to ensure quality in the areas of instrumental drift. The total digestion method as described above can be found on the Activation Labs website and their literature.

Thermal ionization mass spectrometry

Approximately 75–100 mg of whole-rock powder was dissolved using a mixture of $HF-HClO_4$ in a Teflon beaker at ~100°C. In many cases, the same procedures were repeated to ensure the total dissolution of the sample. Strontium and rare earth elements (REEs) were separated using polyethylene columns with a 5 ml resin bed of AG 50W-X8, 200–400 mesh. Neodymium was separated from other REEs using polyethylene columns with an Ln resin as a cation exchange medium. Strontium was loaded on a single Ta-filament with H_3PO_4 and Nd was loaded with H_3PO_4 on a Re-double-filament. $^{143}Nd/^{144}Nd$ ratios were normalized to $^{146}Nd/^{144}Nd = 0.7219$ and $^{87}Sr/^{86}Sr$ ratios to $^{86}Sr/^{88}Sr = 0.1194$. Sr isotopic ratios were measured using a Finnigan MAT-262 thermal ionization mass spectrometer (TIMS), while Nd isotopic ratios were measured using a Finnigan Triton TIMS in the Mass Spectrometry Laboratory, Institute of Earth Sciences, Academia Sinica, Taipei. The $2\sigma_m$ values for all samples are less than or equal to 0.000017 for $^{87}Sr/^{86}Sr$ and less than or equal to 0.000006 for $^{143}Nd/^{144}Nd$. The measured isotope ratio during analyses for JMC Nd standard is 0.511813 ± 0.000010 ($2\sigma_m$) and for NBS987-Sr is 0.710248 ± 0.00001 ($2\sigma_m$). The results can be found in Table 3.

Results

Major and trace elemental data

The major element data recalculated on an anhydrous basis for the samples collected in this study indicate there are three rock types: basalt, basaltic andesite, and andesite (Figure 3a). The basalt is compositionally similar to high-Al (i.e. Al_2O_3 >16.5 wt% and MgO <7 wt%) tholeiites, has a Mg# of 55.5, and the highest TiO_2 ($TiO_2 = 1.5$ wt%) content of all rocks in the study. The basaltic andesites are calc-alkaline and have a relatively wide compositional range ($SiO_2 = 54.2–56.9$ wt%, $Al_2O_3 = 17.1–21.3$ wt%, $Fe_2O_3t = 7.5–8.6$ wt%, MgO = 3.2–5.4 wt%, CaO = 4.9–9.2 wt%, $Na_2O = 1.9–2.9$ wt%, and $K_2O = 1.1–1.9$ wt%). The three andesite samples are calc-alkaline, medium K_2O, and have Mg# values between 47 and 48 (Figure 3b, c).

The concentration of many transition metals and Ga are typically the highest in the basalt (i.e. Sc = 40 ppm, Co = 29.8, Ni = 27 ppm, Cu = 175 ppm, Ta = 0.7 ppm, Hf = 2.2 ppm, Zn = 88.8 ppm, Y = 20.7 ppm, Zr = 76 ppm, Ga = 19.6 ppm) and decrease in the basaltic andesites and andesites, although the basaltic andesites have the highest V (i.e. V = 210 to 270 ppm) and Cr (i.e. Cr = 13–96 ppm). The Rb, Sr, and Ba contents are not significantly different between all rock types. The primitive mantle normalized trace element diagrams of the rocks show similar patterns, with distinct depletions of Nb-Ta and Ti and enrichment of Cs and other large-ion lithophile elements (LILEs) such as Rb and Ba, although Nb-Ta and Ti depletion is less pronounced in the basalt samples (Figure 4a, c, e). There are few discernible differences between the basaltic andesites and andesites as their chondrite normalized REE patterns are light REE (LREE)

Table 2. Major and trace elemental data of rocks from the Tatun volcanic group.

Sample	166	190	T-160	227	230	229	224	223a	T-223	T-210	249	T-309
SiO_2 (wt%)	59.71	59.58	57.72	56.17	54.07	56.12	56.44	49.88	52.04	56.53	56.91	51.27
TiO_2	0.52	0.52	0.51	0.56	0.60	0.54	0.55	0.59	0.59	0.64	0.61	1.51
Al_2O_3	18.81	18.84	18.41	17.13	17.96	16.56	17.54	19.01	19.39	19.62	17.96	17.40
Fe_2O_3t	6.41	6.43	6.63	7.82	8.38	7.45	7.50	7.74	7.69	7.69	7.68	9.53
MnO	0.13	0.14	0.14	0.14	0.15	0.14	0.14	0.15	0.15	0.15	0.14	0.16
MgO	2.90	2.99	2.97	5.00	5.33	5.16	4.73	4.43	4.47	3.26	3.74	6.01
CaO	7.39	7.27	7.54	9.05	9.20	8.99	8.50	4.36	6.65	8.15	8.07	10.18
Na_2O	2.97	2.96	2.90	2.48	2.35	2.42	2.50	1.69	2.21	2.88	2.70	2.37
K_2O	1.46	1.45	1.56	1.54	1.37	1.65	1.64	1.34	1.12	1.14	1.89	1.41
P_2O_5	0.18	0.18	0.19	0.24	0.15	0.26	0.24	0.24	0.24	0.20	0.28	0.26
LOI	0.40	0.64	0.97	0.34	1.15	2.23	0.99	10.37	5.92	0.93	0.78	0.55
Total	100.91	101.00	99.54	100.47	100.82	101.52	100.77	99.80	100.47	101.19	100.76	100.65
Mg#	47.3	47.9	47.0	55.9	55.8	57.8	55.5	53.1	53.5	45.6	49.1	55.5
Sc (ppm)	19	20	20	34	38	37	33	32	35	23	29	40
V	183	187	179	249	274	246	246	249	248	208	231	144
Cr	16.0	13.5	12.1	82.5	60.8	95.6	61.4	46.6	58.6	12.9	17.3	64.6
Co	14.3	14.7	14.0	24.5	26.7	23.6	23.0	21.4	20.9	17.9	20.7	29.8
Ni	9.1	7.1	6.7	17.6	18.3	18.8	16.0	12.6	13.6	6.3	12.2	27.0
Cu	58.4	39.5	46.8	75.5	101	78.2	107	50.2	49.8	62.4	98.2	175
Zn	68.9	68.8	65.4	71.2	81.6	67.7	69.3	73.6	71.7	83.8	72.4	88.8
Ga	16.9	16.7	16.1	15.7	15.0	15.0	15.8	17.7	17.3	18.2	15.8	19.6
Rb	54.2	55.8	59.1	68.4	46.7	75.9	70.8	37.1	22.7	41.1	67.7	58.7
Sr	343	360	365	431	456	440	430	181	319	375	460	419
Y	13.4	14.3	13.1	14.2	15.9	13.9	13.8	15.1	11.0	18.2	15.0	20.7
Zr	61	59	63	59	63	51	62	69	67	67	70	76
Nb	3.4	3.5	3.7	2.9	3.0	3.0	3.1	4.0	4.2	2.6	3.7	0.4
Cs	3.2	3.3	5.1	3.9	4.1	3.8	5.4	1.9	3.9	2.7	2.6	3.6
Ba	411	407	415	365	386	376	420	426	431	345	463	410
La	11.3	12.9	12.5	11.9	13.2	12.7	12.9	13.6	10.9	12.5	14.8	17.5
Ce	23.6	26.0	24.7	24.1	24.2	23.6	25.2	28.1	21.5	25.5	27.9	38.1
Pr	2.8	3.2	2.9	2.9	3.1	2.9	3.1	3.5	2.6	3.2	3.6	4.9
Nd	10.9	12.5	11.3	11.9	12.5	11.7	11.8	13.7	10.3	13.2	14.4	20.8
Sm	2.4	2.6	2.3	2.5	2.6	2.4	2.5	2.9	2.1	3.0	3.0	4.5
Eu	0.79	0.84	0.73	0.82	0.89	0.81	0.83	0.92	0.68	0.98	0.95	1.47
Gd	2.8	2.9	2.7	3.0	3.2	2.7	2.9	3.2	2.4	3.4	3.3	5.0
Tb	0.4	0.5	0.4	0.5	0.5	0.4	0.4	0.5	0.4	0.5	0.5	0.7
Dy	2.9	3.0	2.6	2.9	3.2	2.8	2.8	3.2	2.4	3.5	3.1	4.5
Ho	0.6	0.6	0.6	0.6	0.7	0.6	0.6	0.7	0.5	0.7	0.6	0.9
Er	1.9	2.0	1.8	2.0	2.0	1.8	1.9	2.1	1.6	2.4	1.9	2.6
Tm	0.3	0.3	0.3	0.3	0.3	0.3	0.3	0.3	0.2	0.3	0.3	0.4
Yb	1.7	1.8	1.6	1.7	1.8	1.6	1.7	1.8	1.4	2.1	1.6	1.9
Lu	0.3	0.3	0.3	0.3	0.3	0.3	0.3	0.3	0.2	0.3	0.3	0.3
Hf	1.8	1.8	1.7	1.7	1.6	1.6	1.8	2.0	1.9	1.8	1.8	2.2
Ta	0.2	0.2	0.2	0.3	0.2	0.2	0.3	0.3	0.3	0.2	0.2	0.7
Th	5.6	6.0	5.9	6.1	6.0	6.0	7.2	8.7	4.8	4.3	5.8	6.3
U	1.6	1.9	1.7	4.8	1.7	1.8	2.2	2.5	2.2	1.1	1.6	1.6
$(La/Yb)_N$	4.8	5.1	5.6	5.0	5.3	5.7	5.4	5.4	5.6	4.3	6.6	6.6
Eu/Eu*	0.93	0.93	0.89	0.91	0.94	0.97	0.94	0.92	0.92	0.93	0.92	0.94

Sample	SDC-1 m.v. (30)	SDC-1 r.v.	DNC-1a m.v.	DNC-1a r.v.	GXR-1 m.v.	GXR-1 r.v.	166 duplicate	BIR-1 m.v. (39)	BIR-1 r.v.
SiO_2 (wt%)	65.73	65.8					59.87	47.75	47.96
TiO_2	0.99	1.01					0.52	0.96	0.96
Al_2O_3	15.89	15.8					18.85	15.42	15.5
Fe_2O_3t	6.76	6.32					6.40	11.16	11.3
MnO	0.11						0.13	0.17	0.175
MgO	1.64	1.69					2.91	9.59	9.70
CaO	1.43	1.40					7.38	13.22	13.3
Na_2O	2.04	2.02					2.97	1.73	1.82

(*Continued*)

Table 2. (Continued).

Sample	SDC-1 m.v. (30)	SDC-1 r.v.	DNC-1a m.v.	DNC-1a r.v.	GXR-1 m.v.	GXR-1 r.v.	166 duplicate	BIR-1 m.v. (39)	BIR-1 r.v.
K_2O	3.22	3.28					1.47	0.03	0.03
P_2O_5	0.14	0.16					0.18	0.02	0.21
LOI	1.56						0.40	−0.28	
Total	99.51						101.09	99.78	
Mg#									
Sc (ppm)	16	17	31	31	<1	1.58	19		
V	72	102	148	148	76	80	185		
Cr	48.9	64	202	270	13.7	12.0	15.7		
Co	17.1	18.0	57.1	57.0	7.6	8.2	14.4		
Ni	33.9	38.0	271	247	38	41	11		
Cu	28	30	95.2	100	1090	1110	59.9		
Zn	108	103	73.2	70.0	814	760	68.7		
Ga	21.3	21.0			9.8	13.8	17.0		
Rb	95.2	127			2.7	14.0	55.6		
Sr	165	180	137	144	276	275	341		
Y			16.2	18.0	27.9	32.0	13.3		
Zr	45	290	35	38	20	38	60		
Nb	6.2	21			0.7	0.8	3.4		
Cs	3.8	4.0			2.62	3.00	3.2		
Ba	575	630	104	118	626	750	417		
La	38.2	42.0	3.7	3.6	7.0	7.5	11.1		
Ce	84.8	93.0			13.9	17.0	23.4		
Pr							2.8		
Nd	37.7	40.0	4.9	5.2	8.0	18.0	10.8		
Sm	7.4	8.2			2.7	2.7	2.4		
Eu	1.62	1.70	0.61	0.59	0.64	0.69	0.79		
Gd	7.8	7.0			4.4	4.2	2.8		
Tb	1.1	1.2			0.8	0.83	0.4		
Dy	6.8	6.7			5.3	4.3	2.8		
Ho	1.4	1.5					0.6		
Er	4.1	4.1					1.9		
Tm	0.60	0.65			0.4	0.43	0.3		
Yb	3.2	4.0	2.0	2.0	2.2	1.9	1.7		
Lu					0.3	0.28	0.3		
Hf	1.0	8.3			0.2	0.96	1.8		
Ta	0.3	1.2					0.2		
Th	12.3	12.0			3.6	2.44	5.4		
U	2.7	3.1			32.5	34.9	1.5		

Notes: LOI = loss on ignition; Mg# = $[Mg^{2+}/(Mg^{2+} + Fe^{2+})]*100$; N = normalized to chrondite values of Sun and McDonough (1989); Eu/Eu* = $[2*Eu_N/(Sm_N + Gd_N)]$. m.v. = measured value, r.v. = recommended value.

enriched, with La/Yb$_N$ ratios between 4.3 and 6.6 and Eu/Eu* values between 0.89 and 0.97 (Figure 4b, d, f).

Sr-Nd isotope geochemistry

Reported $^{40}A/^{39}Ar$ and $^{40}K/^{39}Ar$ date ages from the volcanic rocks of the TTVG range from 0.2 to 1.5 Ma (Wang et al. 2004). We chose the youngest age (i.e. 200 ka) to calculate the initial Sr-Nd isotope ratios due to the relative consistency between ^{40}Ar-^{39}Ar and ^{40}K-^{39}Ar dates; however, we noted that calculating the maximum age range represents an insignificant difference in the value. All rock types have similar initial $^{87}Sr/^{86}Sr$ values (I$_{Sr}$ = 0.70414–0.70488). Much like I$_{Sr}$ values, initial $^{143}Nd/^{144}Nd$ ratios for the TTVG rocks are relatively restricted and range from

0.51275 to 0.51279, which corresponds to εNd$_{(T)}$ values of +2.2 to +3.1 using a CHUR value of 0.512639 (Figure 5).

Discussion

Intra-continental origin of the tholeiite basalt

The basaltic rocks from the NTVZ, including rocks from the TTVG, were extensively studied by Wang et al. (2004), who concluded that the basaltic rocks were generated by mixing between asthenospheric mantle melts and enriched, garnet-bearing subcontinental lithospheric mantle (SCLM) melts within a post-collisional extensional environment, with inconsequential contamination from crustal sources at ≤2 Ma. The SCLM end-member source

Table 3. Whole-rock Sr and Nd isotope data for Tatun volcanic group rocks.

Sample	Rock	Rb (ppm)	Sr (ppm)	$^{87}Rb/$ ^{86}Sr	$^{87}Sr/$ ^{86}Sr	$2\sigma_m$	I_{Sr}	Sm (ppm)	Nd (ppm)	$^{147}Sm/$ ^{144}Nd	$^{143}Nd/$ ^{144}Nd	$2\sigma_m$	$\varepsilon Nd_{(T)}$	f (Sm/ Nd)	T_{DM}-1 (Ma)
166	Andesite	54.2	343	0.457	0.70468	17	0.70468	2.4	10.9	0.1331	0.51275	6	+2.2	−0.32	757
190	Andesite	55.8	360	0.448	0.70489	14	0.70488	2.6	12.5	0.1257	0.51275	6	+2.3	−0.36	688
T-160	Andesite							2.3	11.3	0.1231	0.51275	7	+2.2	−0.37	674
227	B-A	68.4	431	0.459	0.70424	9	0.70424	2.5	11.9	0.1270	0.51279	6	+3.1	−0.35	625
230	B-A	46.7	456	0.296	0.70417	11	0.70416	2.6	12.5	0.1257	0.51278	6	+2.7	−0.36	644
229	B-A	75.9	440	0.499	0.70414	12	0.70414	2.5	11.8	0.1281	0.51278	5	+2.7	−0.35	670
224	B-A	70.8	430	0.476	0.70423	9	0.70423	2.5	11.8	0.1281	0.51277	6	+2.6	−0.35	679
223a	B-A	37.1	181	0.593	0.70433	9	0.70433	2.9	13.7	0.1280	0.51275	5	+2.3	−0.35	705
T-223	B-A	22.7	319	0.206	0.70444	11	0.70444	2.1	10.3	0.1233	0.51276	6	+2.3	−0.37	663
T-210	B-A	41.1	375	3.170	0.70475	13	0.70475	3.0	13.2	0.1374	0.51275	6	+2.2	−0.30	800
249	B-A	67.7	460	0.426	0.70442	12	0.70442	3.0	14.4	0.1260	0.51275	6	+2.2	−0.36	697
T-309	Basalt	58.7	419	0.405	0.70445	14	0.70445	4.5	20.8	0.1308	0.51278	6	+2.7	−0.34	688

Notes: B-A, basaltic andesite. Rb, Sr, Sm and Nd concentrations were obtained by ICP-MS and precisions better than ±2%. The results of isotopic measurements for Sr and Nd reference materials are NBS-987 (Sr) = 0.710248 ± 3 (2σm). JMC (Nd) = 0.511813 ± 10 (2σm). f(Sm/Nd) is defined as $((^{147}Sm/^{144}Nd)/0.1967-1)$. $\varepsilon Nd_{(T)}$ is calculated using an approximate equation of $\varepsilon Nd_{(T)} = \varepsilon Nd_{(0)}-Q*f*T$, in which Q = 25.1 Ga^{-1}, f = f(Sm/Nd), and T age = 200 ka. $T_{DM}-1 = (1/\lambda)*ln[1 + ((^{143}Nd/^{144}Nd)_m-0.51315)/((^{147}Sm/^{144}Nd)_m-0.2137)]$; λ = 0.00654 Ga^{-1}.

was probably affected by subduction-related metasomatism within the old Ryukyu arc (i.e. ≥2.6 Ma) prior to the opening of the Okinawa trough because the Sr-Nd-Pb isotopes and low Ce/Pb ratios (i.e. <8) of the basalts are more depleted than would be expected from sediment contamination alone (Ayers 1998; Chung *et al.* 2001; Wang *et al.* 2004). The mixing proportion of the melt from the SCLM to the asthenospheric mantle melt is estimated to be between 20 and 30% for the basalts from TTVG and the neighbouring Kuanyinshan volcanic group. The basalts from TTVG and Kuanyinhsan are thought to contain the highest proportion of SCLM-derived melts within NTVG, which may be related to the fact that the volcanic edifices formed on top of the basement rocks of Taiwan rather than within the Ryukyu arc (Figure 1).

There is one basalt sample (i.e. 309) in this study from TTVG and it is chemically similar to the TTVG data presented by Wang *et al.* (2004). The data show the basaltic rocks from the TTVG to be compositionally similar to tholeiitic, within-plate continental basalts (Figure 6). The precise petrogenetic origin may be debated but the geochemical evidence indicates that these basalts are more similar to those found at within-plate settings than at island-arc settings. The Nb-Ta depletion observed in the primitive mantle normalized incompatible element plot and the moderately depleted Nd isotopes (i.e. $\varepsilon Nd_{(T)}$ = +2.7) are consistent with the model proposed by Wang *et al.* (2004).

Mantle origin of the basaltic andesites

The basaltic andesites are calc-alkaline, have moderate to high Mg# (46–58), and are considered to be derived either from basalt by fractional crystallization or by direct partial melting of an enriched SCLM mixed with asthenosphere-derived melts (Lo 1982; Wang *et al.* 2004). The major element plots show that there is a compositional trend from the basalts through the basaltic andesites to the andesites and may be supportive of the fractionation hypothesis. The most distinctive trend is seen on the plots of TiO_2 vs. Fe_2O_3t or SiO_2, where there is a noticeable inflection just as the bulk composition changes from basalt to basaltic andesite (Figures 7 and 8a). However, the compositional trend may not indicate fractional crystallization and could be an artefact of partial melting with or without crustal contamination.

In order to test the fractional crystallization hypothesis we applied thermodynamic modelling using the petrological software MELTS (Ghiorso and Sack 1995; Smith and Asimow 2005). The MELTS program allows the user to test different fractionation models using a fixed starting composition within the SiO_2-TiO_2-Al_2O_3-Fe_2O_3-Cr_2O_3-FeO-MnO-MgO-CaO-Na_2O-K_2O-P_2O_5-H_2O system, initial pressure (bars), water content (wt%), and relative oxidation state (AO_2). Models were run using starting compositions equal to the TTVG basalt, pressure range of 0.1−5 kbar, oxidation conditions between FMQ −2 and FMQ +3, and water contents between saturation and anhydrous. None of the possible combinations of the parental magma composition or conditions could reproduce the observed basaltic andesite composition; in particular the TiO_2 content of the resultant models is always too high for the given SiO_2 content. Furthermore, some of the basaltic andesites have higher Mg# but the same $\varepsilon Nd_{(T)}$ values as the basalts, implying that the former cannot be derived from the same magma batch. Therefore it is unlikely that the basaltic andesites are derived by fractional crystallization of a basaltic parental magma.

Silicic magmas can be generated directly from the mantle providing that it has been hydrated and/or reacted with silicic melts from subducted crust to form pyroxenite (Rapp *et al.* 1999; Straub *et al.* 2008, 2011). The silicic magmas can range in composition from basaltic andesite to dacite and commonly have high Mg# (>50), Sr/Y ≤ 33, and Gd/Yb < 3,
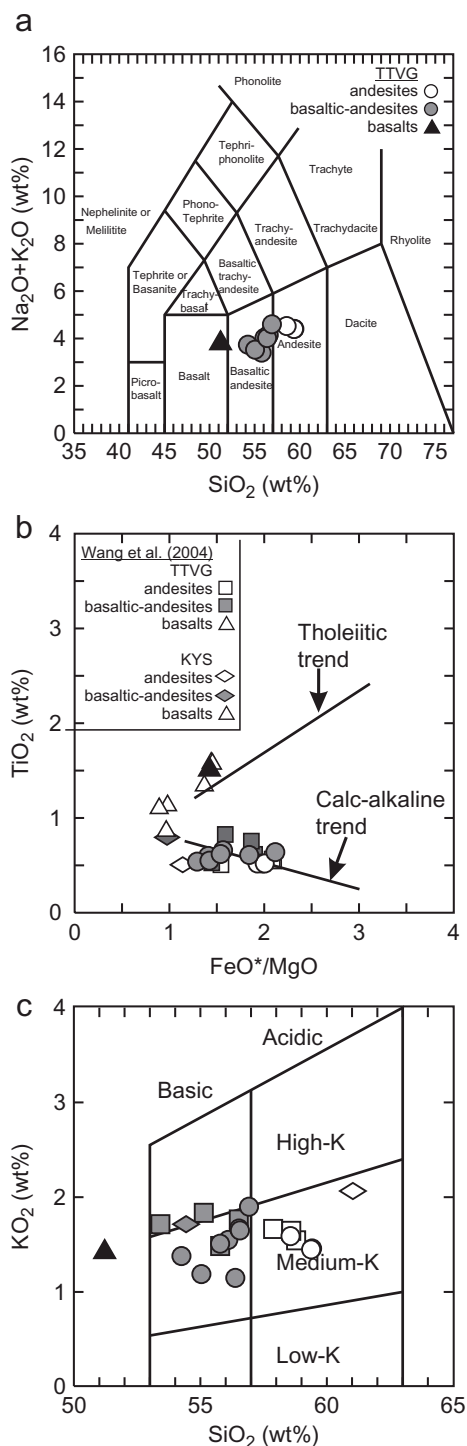
Figure 3. Classification of the Tatun volcanic group rocks. (a) Total alkalies ($Na_2O + K_2O$ wt%) vs. SiO_2 (wt%) normalized to 100% (BAS *et al.* 1986). (b) Discrimination of the tholeiitic basalts from the calc-alkaline basaltic andesites and andesites (Miyashiro 1974). (c) Classification of andesitic rocks (Gill 1981). Additional data from Wang *et al.* (2004).

with Nd and He isotopes more similar to MORB than enriched (i.e. crust, subducted sediment) sources as well as

high Ni olivine (Sobolev *et al.* 2005; Straub *et al.* 2008, 2011). The TTVG basaltic andesites have Sr/Y values <33 (Sr/Y = 12–32) and Gd/Yb ratios <3 (Gd/Yb = 1.6–2.6), but Mg# ranges from 44 to 57 and Nd isotopes are between 0.51275 and 0.51279. The high-Mg# basaltic andesites are, in some cases, more primitive than the basalts from the same edifice. The highest-Mg# rocks may be direct partial melts from a mantle source whereas the lower-Mg# rocks may have experienced some fractionation of mafic silicate minerals (i.e. clinopyroxene) prior to emplacement (Wang *et al.* 2002). Additionally, LILE enrichment and Nb-Ta depletion are observed within the basalts and basaltic andesites, and the fact that both rock types have similar isotope compositions suggests the basaltic andesites are derived from the same isotopic reservoir as the basalts; however, they may be from different mantle lithologies.

It is possible that during the pre-extensional subduction environment, the SCLM beneath Taiwan was enriched by silicic fluids derived from the downgoing slab and created pyroxenite-rich regions within the mantle. These pyroxenite-rich regions could be a source of the basaltic andesites (Straub *et al.* 2011). The proposed model of basalt genesis described by Wang *et al.* (2004) suggests that asthenospheric melts are injected into the enriched SCLM as the Okinawa Trough opens. Melts derived by mixing between the pyroxenite-rich and asthenospheric mantles may be able to produce the basaltic andesites, whereas the ambient SCLM and asthenospheric melts produced the basalts. The lower TiO_2 concentration of the basaltic andesites in comparison with some of the basalts may be related to the hydrated/silicified nature of the pyroxenite regions and the expansion of the stability field of Ti-rich accessory minerals such as titanite and rutile (Hellman and Green 1979; Green 1981; Tatsumi 1989). We suggest that the ambient SCLM was affected less by widespread hydration and silification and therefore would not have permitted stabilization of Ti-bearing minerals, thus allowing for the generation of higher-Ti and lower-silica melts (i.e. sample 309).

Fractionation (and assimilation) origin of andesite from basaltic andesite

The andesites from the TTVG are considered to be derived by fractional crystallization of a more mafic parental magma, but beyond Harker diagrams there is limited robust evidence for their origin (Lo 1982; Wang *et al.* 2004). We apply MELTS modelling using one of the most primitive basaltic andesites (i.e. 230) as the parental magma starting composition. The relative oxidation status of the parental magma is constrained by measurements from volcanic fluids within rocks from Tatun (Ohba *et al.* 2010). The results of Ohba *et al.* (2010) show that relative oxidation status ranges from relatively reducing to relatively oxidizing. The fluids indicative of a reducing environment were characterized as having intimate interaction with the crust
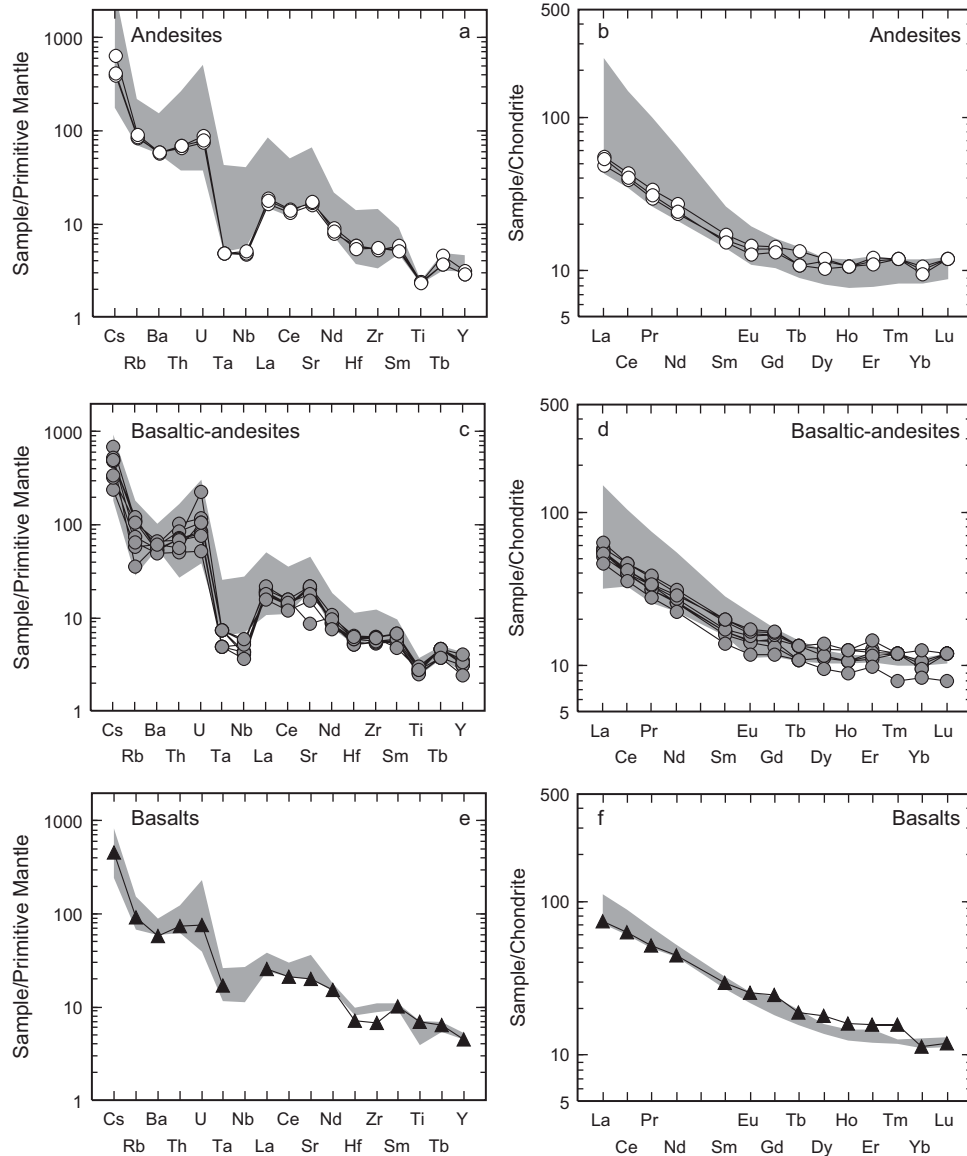
Figure 4. Normalized incompatible element diagrams of rocks from the Tatun volcanic group. Primitive mantle normalized diagrams of the andesites (a), basaltic andesites (c), and basalts (e). Chrondrite normalized diagrams of the andesites (b), basaltic andesites (d), and basalts (f). Normalizing values from Sun and McDonough (1989). Shaded areas represent the range of data according to Wang *et al.* (2004).

and a long residency time whereas the presence of relatively oxidizing fluids is more indicative of a MORB origin, and thus we chose an oxidation status that is more oxidizing (i.e. FMQ +1). The remaining parameters (i.e. initial water content and pressure) were determined by trial and error. The model that produced the best results was water saturated (i.e. $H_2O \approx 2.5\%$) at a pressure equal to 750 bars (i.e. ~2 km depth). The conditions are geologically reasonable given that there are currently emissions of volcanic gases (i.e. H_2S and SO_2) and active hot springs within the Yangmingshan national park area of the TTVG (Lee *et al.* 2005).

The shallow-pressure model calculations show that olivine (Fo_{82}) first appears on the solidus at a temperature of 1105°C, followed by diopside-augite at 1085°C. As soon as clinopyroxene starts to crystallize the olivine stops crystallizing until the temperature reaches 1055°C, just before (i.e. 1060°C) plagioclase (An_{84}) and at the same temperature (i.e. 1065°C) that apatite begins to crystallize. The next mineral to crystallize is Fe-Ti-rich spinel at 1050°C. The crystallizing mineral assemblage remains stable until 1045°C, when olivine (Fo_{78}) stops crystallizing and orthopyroxene starts. The bulk composition similar to most of the andesites at Tatun is reached at ~1030°C after ~32% crystallization of the parental
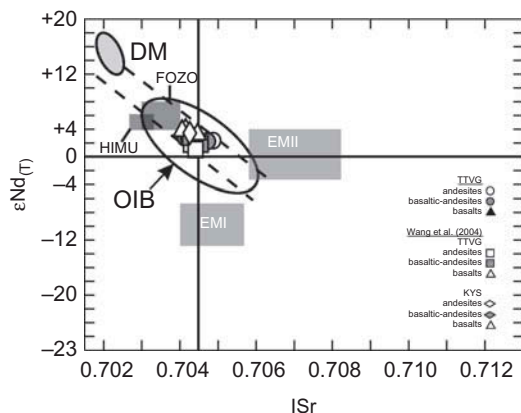
Figure 5.　Sr-Nd plot of rock from the Tatun volcanic group. DM, depleted mantle; EMI, enriched mantle I; EMI, enriched mantle II; HIMU, high µ; FOZO, focus zone (Zindler and Hart 1986; Hart *et al.* 1992; Campbell 2007). Additional data from Wang *et al.* (2004).
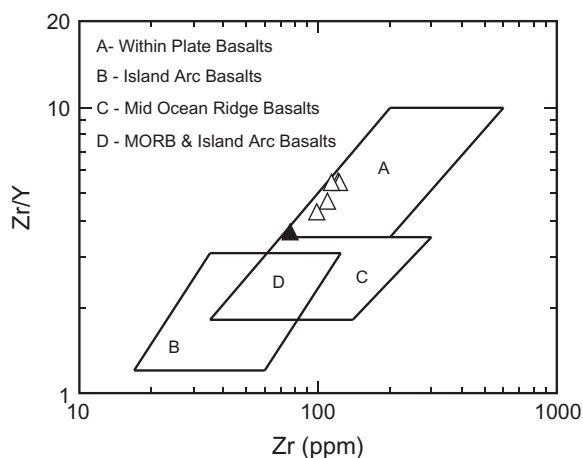

Figure 6.　Tectono-magmatic discrimination diagram of Pearce and Norry (1979) of basalts from the Tatun volcanic group. Additional data from Wang *et al.* (2004).

magma. The fractionating mineral assemblage at 1030°C is orthopyroxene, clinopyroxene, plagioclase (An_{79}), spinel, and apatite. The anhydrous modelled liquid evolution curves are plotted in Figure 8. In nearly all cases the modelled curves pass immediately through or in close proximity to the measured compositions of the andesites from this study and those previously reported. The only element that is not well replicated in the modelled curves is MnO. However, Mn has no effect on the liquid line of descent because it does not partition into the major rock-forming minerals in this system. Although there is inherent uncertainty in the precise starting composition and initial magmatic conditions, the modelled results support the fractionation hypothesis that the andesites very likely formed by shallow (~2 km), hydrous crystal fractionation of a basaltic andesite parental composition.
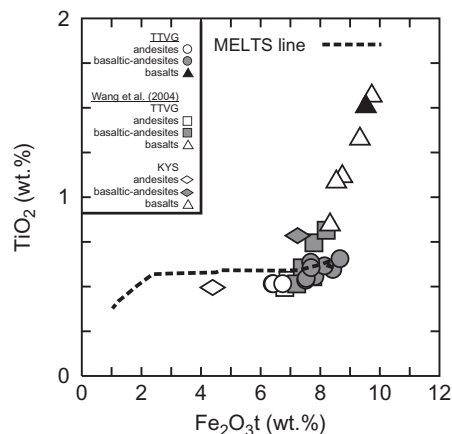
Figure 7.　TiO_2 (wt%) vs. Fe_2O_3t (wt%) with mass balance fractionation and MELTS liquid evolution curves. All data are normalized to 100%. Additional data from Wang *et al.* (2004).

Crustal contamination may play a role in genesis of the andesites because the relationship between MgO and the I_{Sr} values indicates a negative correlation for the rock suite at Tatun (Figure 9). It is possible that the source is isotopically heterogeneous given that it was likely affected by mixing between the SCLM and the asthenosphere. However, the initial $^{143}Nd/^{144}Nd$ ratios do not vary substantially ($^{143}Nd/^{144}Nd_i$ = 0.51275–0.51279), suggesting they may not be as sensitive to crustal assimilation as the I_{Sr} values. If we consider that the Nd isotopes are less sensitive to crustal assimilation than the Sr isotopes and that there is some source heterogeneity, then it is reasonable to conclude that samples with the same Nd isotope composition and differing Sr isotope composition are reflecting differences in crustal contamination rather than source heterogeneity. If that is the case then isotope-mixing calculations indicate that ≤2% crustal contamination is needed, assuming a crustal component similar to the Cenozoic metasedimentary rocks in the region (i.e. I_{Sr} = 0.72030; Sr = 95 ppm), to explain the isotope variation between the parental basaltic andesite (i.e. I_{Sr} = 0.70443; $^{143}Nd/^{144}Nd_i$ = 0.51275) and the daughter andesitic magmas (i.e. I_{Sr} = 0.70488; $^{143}Nd/^{144}Nd_i$ = 0.51275) (Lan *et al.* 2002). Therefore we suggest that crustal contamination likely occurred but that it was a relatively insignificant petrochemical process during genesis of the andesites.

Relationship between TTVG and Kuanyinshan volcano

The results of petrological modelling indicate that the TTVG andesitic rocks are likely derived by fractional crystallization of basaltic andesite magma. Less than 5 km to the southeast of TTVG is the Kuanyinshan (KYS) volcano. KYS is currently considered a separate volcanic system from TTVG and there have been few, if any, suggestions that they are directly related. The KYS
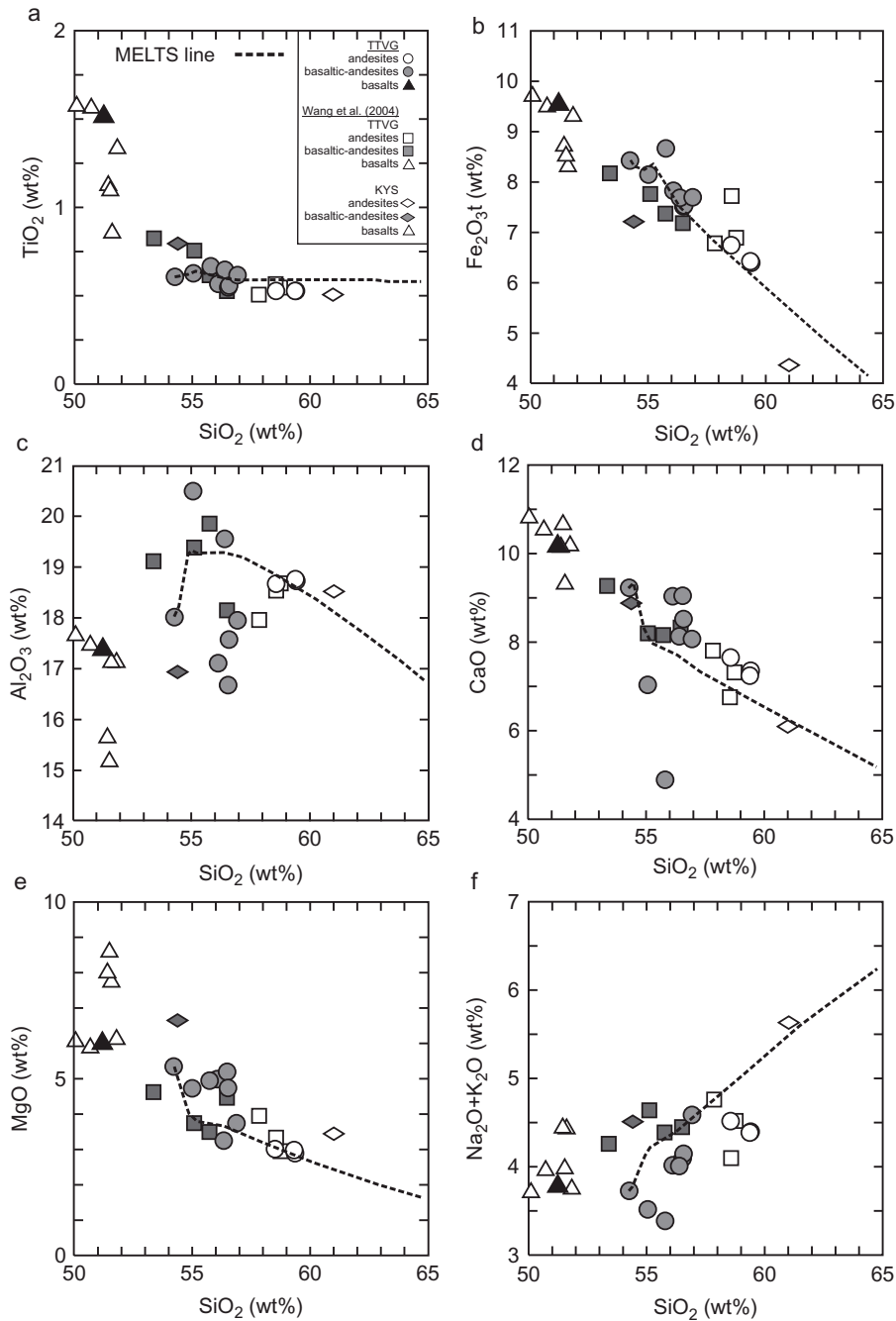
Figure 8. Harker diagrams with mass balance fractionation and liquid evolution curves. (a) Al_2O_3 (wt%) vs. SiO_2 (wt%); (b) CaO (wt%) vs. SiO_2 (wt%); (c) TiO_2 (wt%) vs. SiO_2 (wt%); (d) Fe_2O_3t (wt%) vs. SiO_2 (wt%); (e) MgO (wt%) vs. SiO_2 (wt%); (f) $Na_2O + K_2O$ (wt %) vs. SiO_2 (wt%). All data are normalized to 100%. Additional data from Wang *et al.* (2004). Symbols are as in Figure 7.

edifice is a composite volcano mainly composed of three successive lava flows and agglomerates and consists of a lowermost clinopyroxene andesite lava flow, a middle two-pyroxene andesite lava flow, and an upper hypersthene hornblende andesite lava flow (Chen and Hwang 1982; Hwang and Lo 1986). Basalt is relatively less abundant and only outcrops to the southeast of the

volcano. The volcanic activity in this area was dated by two different methods, $^{40}K/^{39}Ar$ and fission-track, and yielded ages between 0.2 and 1.1 Ma (Juang and Chen 1989; Wang 1989). Chen (1982) described most of the volcanic rocks as porphyritic with phenocrysts consisting of zoned plagioclase, olivine, augite, hypersthene, amphibole, and biotite, and proposed that the KYS andesites
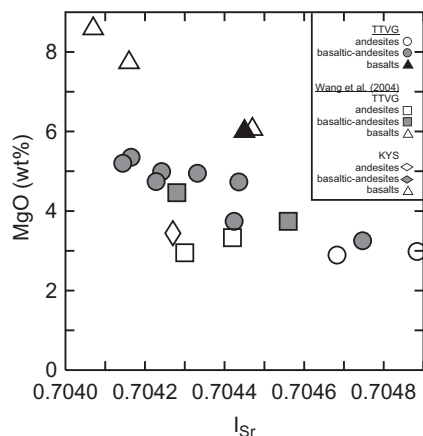
Figure 9. MgO (anhydrous) vs. I_{Sr} ratio of rocks from TTVG and KYS.

Figure 10. Conceptual cogenetic tectonic model of rocks from the Tatun volcanic group and Kuanyinshan group.

were likely derived from basalts through fractionation of an amphibole ± plagioclase ± magnetite assemblage; whereas Hwang and Lo (1986) suggested that there are three differentiation trends with different fractionates consisting of amphibole, plagioclase, or magnetite. Crystal fractionation was supported by the trace element distribution described by Chen (1990). Wang *et al.* (2004) pointed out that the nascent KYS high-K calc-alkaline/shoshonitic basalt is more enriched with LILEs and LREEs among the NTVZ volcanics and originated from a low degree of partial melting from asthenoshperic mantle mixed with a higher proportion of metasomatized SCLM.

Because the volcanic rocks at KYS and TTVG have very similar bulk compositions and their petrogenetic models are also very similar, we propose that both volcanic groups are tapping the same mantle system (Figures 3, 5, 6, 7, 8). Figure 10 shows a possible scenario for the development of the KYS-TTVG system. The first stage is the injection of mafic magmas into the crust directly from the source. Some of the mafic magmas may directly erupt to produce the basaltic lavas, whereas other magma batches reach neutral buoyancy and form small magma chambers (not shown). The basaltic andesite magmas may erupt directly from the mantle source or fractionate in shallow magma chambers to produce the andesitic magmas. Because of the compositional similarity of the basalts between the two volcanic systems it is very likely that the magmas originate from the same source. Our proposed petrogenetic model is based on the close spatial associations and geochemical similarities between TTVG and KYS but it does not confirm that the two volcanic edifices are tapping the same magma chamber, merely that they originated from the same mantle source. Further geophysical investigations may be able to delineate the presence and possible distribution of crustal-level magma chambers in the region and help provide structural constraints.
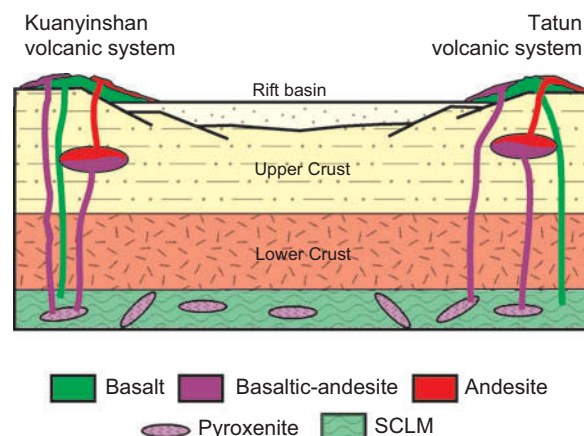
Implications for the Tatun volcanic group

Co-genesis of the basalt and basaltic andesite-andesite has important implications for the development of the NTVZ and circum-Pacific andesites. The basalts from the TTVG are continental tholeiites that were likely derived by mixing of SCLM melts and asthenospheric melts in an extensional environment and not related to an island-arc tectonic system, but rather a back-arc/post-collisional setting (Wang *et al.* 2004). Unlike the eastern portion of the NTVZ, the western portion is exclusively continental in nature and therefore the magmas erupted within thicker crust and had an opportunity to interact with the continental crust (Chen 1965). Consequently the likelihood that shallow (i.e. ~2 km) crustal magma chambers would develop is increased. The fact that there are only a few basaltic flows within the predominantly andesitic volcanic system could be related to the basaltic magmas stalling in the crust prior to eruption. Furthermore if the andesitic rocks are the result of differentiation of the basaltic andesite magmas, then only the residual liquids would be expected to erupt.

In comparison with other regions (i.e. Japan, Cascades, Aleutians) of the circum-Pacific volcanic zone, the Tatun andesites may be unique in the sense that they were not generated within the confines of a subduction zone and were rather formed by fractionation of mafic melts from a mixed SCLM-asthenopsheric mantle source within a tensional setting (Chung *et al.* 2001; Wang *et al.* 2004). The negative Nb-Ta anomaly observed in the rocks is likely due to the modification of the subcontinental lithospheric mantle during pre-Quaternary subduction along the east Eurasian margin. The relatively complicated tectonic setting (i.e. trench-arc-back-arc basin-oblique arc-continent collision) may favour the formation of an extensional setting, or at least decompression, due to the rapid rate of mountain building and collapse found in Taiwan (Teng 1996). Thus the andesites of the TTVG are likely an

example of shallow-level fractionation of mafic magma under water-saturated and relatively oxidizing conditions (Osborn 1959; Zellmer *et al.* 2005; Shellnutt and Zellmer 2010).

Conclusions

The basalt, basaltic andesites, and andesites of the TTVG represent a co-genetic suite of volcanic rocks formed within an extensional tectonic setting. Back-arc extension associated with the opening of the Okinawa trough is continuous into the northern portion of Taiwan. The extensional setting was sufficient to induce partial melting of subduction-modified SCLM and allow mixing with upwelling asthenospheric melts to produce the basalt and basaltic andesite of the TTVG. The basaltic andesites are likely derived directly by partial melting of a pyroxenetic mantle source, whereas the andesites are derived by fractionation of the basaltic andesites at relatively low pressure (750 bar), water saturation (H_2O = 2.5 wt%), and oxidizing conditions (AO_2 = FMQ +1). The chemical similarity of the TTVG volcanic rocks with the neighbouring Kuanyinshan volcanic rocks suggests that they may share a common petrogeneitc history. The results of this study indicate that some andesitic rocks are generated by shallow-level crystal fractionation of a mafic parental magma within continental portions of back-arc/post-collisional settings.

Acknowledgements

Funding

References

Arculus, R.J., 1994, Aspects of magma genesis in arcs: Lithos, v. 33, p. 189–208. doi:10.1016/0024-4937(94)90060-4

Ayers, J., 1998, Trace element modeling of aqueous fluid-peridotite interaction in the mantle wedge of subduction zones: Contributions to Mineralogy and Petrology, v. 132, p. 390–404.

Bas, M.J., Maitre, R.W., Streckeisen, A., and Zanettin, B., 1986, A chemical classification of volcanic rocks based on the total alkali silica diagram: Journal of Petrology, v. 27, p. 745–750. doi:10.1093/petrology/27.3.745

Belousov, A., Belousova, M., Chen, C.-H., and Zellmer, G.F., 2010, Deposits, character and timing of recent eruptions and gravitational collapses in Tatun volcanic group, northern Taiwan: Hazard-related issues: Journal of Volcanology and Geothermal Research, v. 191, p. 205–221. doi:10.1016/j.jvolgeores.2010.02.001

Boettcher, A.L., 1973, Volcanism and orogenic belts — The origin of andesites: Tectonophysics, v. 17, p. 223–240. doi:10.1016/0040-1951(73)90004-8

Bryan, S., 2007, Silicic large igneous provinces: Episodes, v. 30, p. 20–31.

Campbell, I.H., 2007, Testing the plume theory: Chemical Geology, v. 241, p. 153–176. doi:10.1016/j.chemgeo.2007.01.024

Chen, C., 1978, Petrochemistry and origin of Pleistocene volcanic rocks from northern Taiwan: Bulletin Volcanologique, v. 41, p. 513–528. doi:10.1007/BF02597384

Chen, C., Burr, G., and Lin, S., 2010, Time of a Near Holocene volcanic eruption in the Tatun Volcano Group, Northern Taiwan: Evidence from AMS radiocarbon dating of charcoal ash from sediments of the Sungshan formation in Taipei Basin: Terrestrial, Atmospheric and Oceanic Sciences, v. 21, p. 611–614. doi:10.3319/TAO.2009.12.11.02(TH)

Chen, C.-H., 1975, Petrological and chemical study of volcanic rocks from Tatun volcano group: Proceedings of the Geological Society of China, v. 18, p. 59–72.

Chen, C.-H., 1982, Petrological and geochemical study of the shoshonitic rock of the Kuanyinshan area, Northern Taiwan: Acta Geologica Taiwanica, v. 21, p. 33–62.

Chen, C.-H., 1990. Igneous rocks in Taiwan, Geology of Taiwan Series 1: Taipei, Central Geological Survey (in Chinese).

Chen, C.-H., Chen, C.-H., Mertzman, S.A., and Shen, J.J.-S., 1999, An unusual late Cenozoic volcanic zone in nothern Taiwan behind the soutehrn Okinawa Trough: Journal of the Geological Society of China, v. 42, p. 593–612.

Chen, C.-H., and Hwang, W.T., 1982, An introduction to volcanology: Science Monthly, v. 3, p. 26–31 (in Chinese).

Chen, C.H., and Teng, L.S., 1997, Extensional collapse of the northern Taiwan mountain belt: Comment and Reply: Geology, v. 25, p. 855–856. doi:10.1130/0091-7613(1997)025<0855:ECOTNT>2.3.CO;2

Chen, P.Y., 1965, On the xenoliths of sandstone and shale in andesite from Chihsingshan, Tatun volcanic group, Taiwan: Proceedings of the Geological Society of China, v. 14, p. 5–20.

Chen, W.S., Yang, C.C., Yang, H.C., and Liu, J.K., 2003, Volcanic landform and sequences of the Tatun volcanoes: Bulletin of Central Geological Survey, v. 16, p. 99–123 (in Chinese).

Chiaradia, M., Muntener, O., and Beate, B., 2011, Enriched Basaltic Andesites from mid-crustal fractional crystallization, recharge, and assimilation (Pilavo Volcano, Western Cordillera of Ecuador): Journal of Petrology, v. 52, p. 1107–1141. doi:10.1093/petrology/egr020

Chung, S.L., Wang, K.L., Crawford, A.J., Kamenetsky, V.S., Chen, C.-H., Lan, C.Y., and Chen, C.H., 2001, High-Mg potassic rocks from Taiwan: Implication for the genesis of orogenic potassic magmas: Lithos, v. 59, p. 153–170.

Chung, S.L., Wang, S.L., Shinjo, R., Lee, C.S., and Chen, C.-H., 2000, Initiation of arc magmatism in an embryonic continental rifting zone of the southernmost part of Okinawa Trough: Terra Nova, v. 12, p. 225–230. doi:10.1046/j.1365-3121.2000.00298.x

Chung, S.L., Yang, T.F., Lee, C.Y., and Chen, C.-H., 1995, The igneous provinciality in Taiwan: Consequence of continental rifting superimposed by Luzon and Ryukyu subduction systems: Journal of Southeast Asian Earth Sciences, v. 11, p. 73–80. doi:10.1016/0743-9547(94)00040-L

Davies, J.W., and Stevenson, D.J., 1992, Physical model of source region of subduction zone volcanics: Journal of

Geophysical Research: Solid Earth, v. 97, p. 2037–2070. doi:10.1029/91JB02571

Deer, W.A., Howie, R.A., and Zussman, J., 1992, An Introduction to rock forming minerals (second edition): Harlow: Longmen, p. 696.

Ernst, W.G., 2010, Subduction-zone metamorphism, calc-alkaline magmatism, and convergent-margin crustal evolution: Gondwana Research, v. 18, p. 8–16. doi:10.1016/j.gr.2009.05.010

Ghiorso, M.S., and Sack, R.O., 1995, Chemical mass transfer in magmatic processes IV: A revised and internally consistent thermodynamic model for the interpolation and extrapolation of liquid-solid equilibria in magmatic systems at elevated temperatures and pressures: Contributions to Mineralogy and Petrology, v. 119, p. 197–212.

Gill, J.B., 1981, Orogenic andesites and plate tectonics: Berlin, Springer, p. 390.

Green, T.H., 1981, Experimental evidence for the role of accessory phases in magma genesis: Journal of Volcanology and Geothermal Research, v. 10, p. 405–422. doi:10.1016/0377-0273(81)90089-5

Hart, S.R., Hauri, E.H., Oschmann, L.A., and Whitehead, J.A., 1992, Mantle plumes and entrainment: Isotopic evidence: Science, 256, v. 517–520. doi:10.1126/science.256.5056.517

Hawkesworth, C., Turner, S., Gallagher, K., Hunter, A., Bradshaw, T., and Rogers, N., 1995, Calc-alkaline magmatism, lithospheric thinning and extension in the basin and range: Journal of Geophysical Research, v. 100, p. 10271–10286. doi:10.1029/94JB02508

Hellman, P.L., and Green, T.H., 1979, The role of sphene as an accessory phase in the high-pressure partial melting of hydrous mafic compositions: Earth and Planetary Science Letters, v. 42, p. 191–201. doi:10.1016/0012-821X(79)90024-4

Hwang, W.T., and Lo, H.J., 1986, Volcanological aspects and the petrogenesis of the Kuanyinshan volcanic rocks, Northern Taiwan: Acta Geologica Taiwanica, v. 24, p. 123–148.

Juang, W.S., 1993, Diversity and origin of Quaternary basaltic magma series in northern Taiwan: Bulletin of the National Museum of Natural Science, v. 4, p. 125–166.

Juang, W.S., and Chen, J.C., 1989, Geochronology and geochemistry of volcanic rocks in the northern Taiwan: Bulletin of Geological Survey, v. 5, p. 31–66.

Kelemen, P.B., 1995, Genesis of high Mg# andesites and the continental crust: Contributions to Mineralogy and Petrology, v. 120, p. 1–19. doi:10.1007/BF00311004

Kelemen, P.B., Hanghoj, K., and Greene, A.R., 2003a, One view of the geochemistry of subduction-related magmatic arcs, with an emphasis on primitive andesite and lower crust, *in* Holland, H.D., and Turekian, K.K. eds., Treaties on geochemistry: Amsterdam, Netherlands, Elsevier, p. 593–659.

Kelemen, P.B., and Yogodzinski, G., 2007, High-magnesian andesite from Mount Shasta: A product of magma mixing and contamination, not a primitive melt: COMMENT AND REPLY: COMMENT: Geology, v. 35, p. e149–e150. doi:10.1130/G24099C.1

Kelemen, P.B., Yogodzinski, G.M., and Scholl, D.W., 2003b, Along-strike variation in lavas of the Aleutian island arc: Implications for the genesis of high-Mg# andesite and the continental crust, *in* Eiler, J. ed., Inside the subduction factory, American Geophysical Union Geophysical Monograph, 138: Washington, D.C., American Geophysical Union, p. 223–274.

Lan, C.-Y., Lee, C.-S., Shen, J.J.-S., Lu, C.-Y., Mertzman, S.A., and Wu, T.-W., 2002, Nd-Sr isotopic compositions and

geochemistry of sediments from Taiwan and their implications: Western Pacific Earth Sciences, v. 2, p. 205–222.

Leclerc, F., Bedard, J., Harris, L.B., McNicoll, V.J., Goulet, N., Roy, P., and Houle, P., 2011, Tholeiitic to calc-alkaline cyclic volcanism in the Roy Group, Chibougamau area, Abitibi greenstone belt – revised stratigraphy and implications for VHMS exploration: Canadian Journal of Earth Sciences, v. 48, p. 661–694.

Lee, H.-F., Yang, T.F., and Lan, T.F., 2005, Fumarolic gas composition of the Tatun volcanic group, northern Taiwan: Terrestrial, Atmospheric and Oceanic Sciences, v. 16, p. 843–864.

Lo, H.H., 1982, Compositions of tatun andesites, northern Taiwan: Journal of Volcanology and Geothermal Research, 13, p. 173–187. doi:10.1016/0377-0273(82)90026-9

Miyashiro, A., 1974, Volcanic rock series in island arcs and active continental margins: American Journal of Science, v. 274, p. 321–355. doi:10.2475/ajs.274.4.321

Ohba, T., Sawam, T., Taira, N., Yang, T.F., Lee, H.F., Lan, T.F., Ohwada, M., Morikawa, N., and Kazahaya, K., 2010, Magmatic fluids of Tatun volcanic group, Taiwan: Applied Geochemistry, v. 25, p. 513–523. doi:10.1016/j.apgeochem.2010.01.009

Osborn, E.F., 1959, Role of oxygen pressure in the crystallization and differentiation of basaltic magma: American Journal of Science, v. 257, p. 609–647. doi:10.2475/ajs.257.9.609

Pearce, J.A., and Norry, M.J., 1979, Petrogenetic implications of Ti, Zr, Y and Nb variations in volcanic rocks: Contributions to Mineralogy and Petrology, v. 69, p. 33–47. doi:10.1007/BF00375192

Poli, S., and Schmidt, M.W., 2002, Petrology of subducted slabs: Annual Review of Earth and Planetary Sciences, v. 30, p. 207–235. doi:10.1146/annurev.earth.30.091201.140550

Rapp, R.P., Shimizu, N., Norman, M.D., and Applegate, G.S., 1999, Reaction between slab-derived melts and peridotite in the mantle wedge: Experimental constraints at 3.8 GPa: Chemical Geology, v. 160, v. 335-356. doi:10.1016/S0009-2541(99)00106-0

Ringwood, A.E., 1974, The petrological evolution of island arc systems: Twenty-seventh William Smith Lecture: Journal of the Geological Society of London, v. 130, p. 183–204. doi:10.1144/gsjgs.130.3.0183

Rudnick, R., and Gao, S., 2003 Composition of the continental crust, *in* Rudnick, R. ed., The crust. treatise on geochemistry: Amsterdam, Elsevier, p. 1–64.

Shellnutt, J.G., and Zellmer, G.F., 2010, High-Mg andesite genesis by upper crustal differentiation: Journal of the Geological Society of London, v. 167, p. 1081–1088. doi:10.1144/0016-76492010-070

Sheth, H.C., Torres-Alvarado, I.S., and Verma, S.P., 2002, What is the 'Calc-alkaline rock series'?: International Geology Review, v. 44, p. 686–701. doi:10.2747/0020-6814.44.8.686

Shinjo, R., 1999, Geochemistry of high Mg andesites and the tectonic evolution of the Okinawa Trough-Ryukyu arc system: Chemical Geology, v. 157, p. 69–88. doi:10.1016/S0009-2541(98)00199-5

Sibuet, J.-C., Hsu, S.-K., Shyu, C.-T., and Liu, C.-S., 1995, Structural and kinematic evolutions of the Okinawa Trough backarc basin, *in* Taylor, B. ed., Backarc Basins: Tectonics and Magmatism, New York, Plenum, p. 343–379.

Sisson, T.W., and Grove, T.L., 1993, Experimental investigations of the role of H2O in calc-alkaline differentiation and subduction zone magmatism: Contributions to Mineralogy and Petrology, v. 113, p. 143–166. doi:10.1007/BF00283225

Smith, P.M., and Asimow, P.D., 2005, Adiabat_1ph: A new public front-end to the MELTS, pMELTS, and pHMELTS models: Geochemistry, Geophysics, Geosystems, v. 6, Q02004, doi:10.1029/2004GC000816.

Sobolev, A.V., Hofmann, A.W., Sobolev, S.V., and Nikogosian, I.K., 2005, An olivine-free mantle source of Hawaiian shield basalts: Nature, v. 434, p. 590–597. doi:10.1038/nature03411

Song, S.-R., Tsao, S., and Lo, H.-J., 2000a, Characteristics of the Tatun volcanic eruptions, north Taiwan: Implications for a cauldron formation and volcanic evolution: Journal of the Geological Society of China, v. 43, p. 361–378.

Song, S.R., Yang, T.F., Yeh, Y.H., Tsao, S.J., and Lo, H.J., 2000b, The Tatun Volcano Group is active or extinct?: Journal of Geological Society of China, v. 43, p. 521–534.

Straub, S.M., Gomez-Tuena, A., Stuart, F.A., Zellmer, G.F., Espinasa-Perena, R., Cai, Y., and Iizuka, Y., 2011, Formation of hybrid arc andesites beneath thick continental crust: Earth and Planetary Science Letters, v. 303, p. 337–347. doi:10.1016/j.epsl.2011.01.013

Straub, S.M., LaGatta, A.B., Martin-Del Pozzo, A.L., and Langmuir, C.H., 2008, Evidence from high Ni olivines for a hybridized peridotite/pyroxenite source for orogenic andesites from the central Mexican volcanic belt: Geochemistry, Geophysics, Geosystems, v. 9, p. n/a–n/a. doi:10.1029/2007GC001583

Sun, -S.-S., and McDonough, W.F., 1989, Chemical and isotopic systematics of oceanic basalts: Implications for mantle composition and processes, *in* Saunders, A.D., and Norry, M.J., Eds., Magmatism in the ocean basins 42, Geological Society of London, Special Publication, p. 313–435. doi:10.1144/GSL.SP.1989.042.01.19

Suppe, J., 1984, Kinematics of arc-continent collision, flipping of subduction, and back-arc spreading near Taiwan: Geological Society of China Memoir, v. 6, p. 131–146.

Tatsumi, Y., 1989, Migration of fluid phases and genesis of basalt magmas in subduction zones: Journal of Geophysical Research, v. 94, p. 4697–4707. doi:10.1029/JB094iB04p04697

Tatsumi, Y., Shukuno, H., Tani, K., Takahashi, N., Kodaira, S., and Kogiso, T., 2008, Structure and growth of the Izu-Bonin-Mariana arc crust: 2. Role of crust-mantle transformation and the transparent Moho in arc crust evolution: Journal of Geophysical Research, v. 113, B02203. doi:10.1029/2007JB005121

Teng, L.S., 1990, Geotectonic evolution of late Cenozoic arc-continent collision in Taiwan: Tectonophysics, v. 183, p. 57–76. doi:10.1016/0040-1951(90)90188-E

Teng, L.S., 1996, Extensional collapse of the northern Taiwan mountain belt: Geology, v. 24, p. 949–952. doi:10.1130/0091-7613(1996)024<0949:ECOTNT>2.3.CO;2

Till, C.B., Grove, T.L., and Withers, A.C., 2012, The beginnings of hydrous mantle wedge melting: Contributions to Mineralogy and Petrology, v. 163, p. 669–688. doi:10.1007/s00410-011-0692-6

Ulmer, P., 2001, Partial melting in the mantle wedge – the role of H2O in the genesis of mantle-derived 'arc-related' magmas: Physics of the Earth and Planetary Interiors, v. 127, p. 215–232. doi:10.1016/S0031-9201(01)00229-1

Wang, K.-L., Chung, S.-L., Chen, C.-H., and Chen, C.-H., 2002, Geochemical constraints on the petrogenesis of high-Mg basaltic andesites from the Northern Taiwan volcanic zone: Chemical Geology, v. 182, p. 513–528. doi:10.1016/S0009-2541(01)00338-2

Wang, K.-L., Chung, S.-L., Chen, C.-H., Shinjo, R., Yang, T.F., and Chen, C.-H., 1999, Post-collisional magmatism around northern Taiwan and its relation with opening of the Okinawa Trough: Tectonophysics, v. 308, p. 363–376. doi:10.1016/S0040-1951(99)00111-0

Wang, K.-L., Chung, S.-L., O'Reilly, S.Y., Sun, -S.-S., Shinjo, R., and Chen, C.-H., 2004, Geochemical constraints for the Genesis of post-collisional magmatism and the geodynamic evolution of the northern Taiwan region: Journal of Petrology, v. 45, p. 975–1011. doi:10.1093/petrology/egh001

Wang, W.H., 1989, The volcanology and fission track dating of Tatun volcanics [Master thesis]: Institute of Geology, National Taiwan University, Taipei.

Zellmer, G.F., Annen, C., Charlier, B.L.A., George, R.M.M., Turner, S.P., and Hawkesworth, C.J., 2005, Magma evolution and ascent at volcanic arcs: Constraining petrogenetic processes through rates and chronologies: Journal of Volcanology and Geothermal Research, v. 140, p. 171–191. doi:10.1016/j.jvolgeores.2004.07.020

Zindler, A., and Hart, S.R., 1986, Chemical geodynamics: Annual Review of Earth and Planetary Sciences, v. 14, p. 493–571. doi:10.1146/annurev.ea.14.050186.002425